

Form factor $\pi^0\gamma^*\gamma$ in lightcone sum rules combined with renormalization-group summation vs experimental data.

C. Ayala^{1,*}, S. V. Mikhailov^{2,**}, A. V. Pimikov^{3,***}, and N. G. Stefanis^{4,****}

¹Department of Physics, Universidad Técnica Federico Santa María, Casilla 110-V, Valparaíso, Chile

²Bogoliubov Laboratory of Theoretical Physics, JINR, 141980 Dubna, Russia

³Institute of Modern Physics, Chinese Academy of Science, Lanzhou 730000, China

⁴Ruhr-Universität Bochum, Fakultät für Physik and Astronomie, Institut für Theoretische Physik II, D-44780 Bochum, Germany

Abstract. We consider the lightcone sum-rule (LCSR) description of the pion-photon transition form factor in combination with the renormalization group of QCD. The emerging scheme represents a certain version of Fractional Analytic Perturbation Theory and significantly extends the applicability domain of perturbation theory towards lower momenta $Q^2 \lesssim 1 \text{ GeV}^2$. We show that the predictions calculated herewith agree very well with the released preliminary data of the BESIII experiment, which have very small errors just in this region, while the agreement with other data at higher Q^2 is compatible with the LCSR predictions obtained recently by one of us using fixed-order perturbation theory.

1 Introduction.

In this work we consider the calculation of the $\pi^0\gamma^*\gamma$ transition form factor (TFF) within the LCSR approach, see, e.g., [1, 2], going beyond fixed-order perturbation theory (FOPT). We use instead the approach worked out in [3], which combines the method of LCSRs, based on dispersion relations, with the renormalization-group (RG) summation, expressed in terms of the formal solution of the Efremov-Radyushkin-Brodsky-Lepage (ERBL) [4, 5] evolution equation. We argued [3] that this procedure gives rise to a particular version of fractional analytic perturbation theory (FAPT) [6, 7] within QCD—see [8, 9] for reviews.

From the calculational point of view, this FAPT-related approach helps avoid the appearance of large radiative corrections to the pion-photon TFF at low/moderate momenta. This is because such terms become small by virtue of the FAPT summation in contrast to the currently known [2] FOPT results (up to the order of $O(\alpha_s^2\beta_0)$). The emergent FAPT/LCSR approach rearranges completely the perturbative QCD corrections turning them into a non-power series of FAPT couplings, see [3, 6, 7], which have no Landau singularities when $Q^2 \simeq \Lambda_{\text{QCD}}^2$. As a result, the domain of applicability of this perturbative expansion is significantly extended towards lower momentum transfers. From the phenomenological point of view, the FAPT/LCSR approach extends the validity range of the TFF predictions below

*e-mail: cesar.ayala@usm.cl

**e-mail: mikhs@theor.jinr.ru

***e-mail: pimikov@mail.ru

****e-mail: stefanis@tp2.ruhr-uni-bochum.de

$Q^2 \leq 1 \text{ GeV}^2$, where the preliminary BESIII data on the pion TFF bear very small error bars [10]. This data regime cannot be reliably assessed using LCSRs within FOPT, showing a tendency to underestimate them below 1 GeV^2 [11].

Consider now the pion-photon transition form factor for two highly virtual photons describing the reaction $\gamma^*(-Q^2)\gamma^*(-q^2) \rightarrow \pi^0$ by assuming that $Q^2, q^2 \gg m_p^2$. Applying factorization, the pion-photon transition form factor $F^{\gamma^*\gamma^*\pi^0}$ can be written in terms of convolutions of perturbatively calculable hard-scattering parton amplitudes $T^{(n)}$ of $\gamma^*\gamma^* \rightarrow q(G_{\mu\nu})\bar{q}$ and pion distribution amplitudes (DAs) $\varphi_\pi^{(n)}$ of nonperturbative nature to get

$$F^{\gamma^*\gamma^*\pi^0}(Q^2, q^2, \mu^2) \sim T^{(2)}(Q^2, q^2, \mu^2; x) \otimes_x \varphi_\pi^{(2)}(x, \mu^2) + \quad (1)$$

$$T^{(4)}(Q^2, q^2, \mu^2; x) \otimes_x \varphi_\pi^{(4)}(x, \mu^2) + \text{inverse-power corr. like twist-6}, \quad (2)$$

where $\otimes \equiv \int_0^1 dx$ and the superscript (n) denotes the twist label. We have adopted the default scale setting by identifying the factorization (label F) and renormalization (label R) scale $\mu_F = \mu_R = \mu$. It is possible to sum the infinite series of the logarithmic corrections associated with the coupling $a_s = \alpha_s(\mu^2)/4\pi$ and the $\varphi_\pi(x; \mu^2)$ renormalization by absorbing them into the new argument of the running coupling $\bar{a}_s(q^2\bar{y} + Q^2y) \equiv \bar{a}_s(y)$ and the ERLB exponent for the DAs, respectively. For further details we refer to the discussion given in Sec. II of [3] and references cited therein. The ERLB exponent accumulates all ERLB evolution kernels $a_s^{k+1}V_k$, while only the coefficient functions $a_s^k\mathcal{T}^{(k)}$ of the parton subprocesses remain in the perturbative expansion of the leading-twist amplitude $T^{(2)}$.

It is useful to consider the twist-two pion DA, as well as the corresponding contribution to the TFF in (1), as an expansion in the conformal basis of the Gegenbauer harmonics $\{\psi_n(x) = 6x\bar{x}C_n^{3/2}(x - \bar{x})\}$,

$$\varphi_\pi^{(2)}(x, \mu^2) = \psi_0(x) + \sum_{n=2,4,\dots}^{\infty} a_n(\mu^2)\psi_n(x), \quad (3a)$$

$$F^{(\text{tw}=2)}(Q^2, q^2) = F_0^{(\text{tw}=2)}(Q^2, q^2) + \sum_{n=2,4,\dots}^{\infty} a_n(\mu^2)F_n^{(\text{tw}=2)}(Q^2, q^2). \quad (3b)$$

At the one-loop level, the next-to-leading-order (NLO) coefficient function is $\mathcal{T}^{(1)}$ and the RHS of Eq. (1) for the twist-two contribution reduces in the $\{\psi_n\}$ basis to

$$F_n^{(\text{tw}=2)}(Q^2, q^2) \xrightarrow{1\text{-loop}} F_{(1)n}^{(\text{tw}=2)} = N_T T_0(y) \otimes_y \left\{ \left[\mathbb{1} + \bar{a}_s(y)\mathcal{T}^{(1)}(y, x) \right] \left(\frac{\bar{a}_s(y)}{a_s(\mu^2)} \right)^{v_n} \right\} \otimes_x \psi_n(x). \quad (4)$$

In the above equation, $T_0(y)$ is the Born term of the perturbative expansion for $T^{(2)}$, while the other used notations mean

$$T_0(y) \equiv T_0(Q^2, q^2; y) = \frac{1}{q^2\bar{y} + Q^2y}; \quad \mathbb{1} = \delta(x - y); \quad N_T = \sqrt{2}f_\pi/3; \quad (5)$$

$$V(a_s; y, z) \rightarrow a_s V_0(y, z); \quad V_0(y, z) \otimes \psi_n(z) = -\frac{1}{2}\gamma_0(n)\psi_n(y); \quad \beta(\alpha) \rightarrow -a_s^2\beta_0, \quad (6)$$

where $a_s\gamma_0(n)$ denotes the one-loop anomalous dimension of the corresponding composite operator of leading twist with $v_n = \frac{1}{2}\frac{\gamma_0(n)}{\beta_0}$. It is important to appreciate that Eq. (4) has no sense for small q^2 even if Q^2 is large. Indeed, the scale argument $q^2\bar{y} + Q^2y$ approaches for $y \rightarrow 0$ the small q^2 regime, so that the perturbative expansion becomes unprotected. Therefore, Eq. (4) cannot be directly applied to the TFF calculation. The situation changes drastically when we apply Eq. (4) to a dispersion relation.

2 Essence of FAPT/LCSRs

The RG summation of all radiative corrections to the TFF in Eq. (4) generates a new contribution to the imaginary part of the spectral density (see for details [3]) relative to the standard version of LCSRs [1, 2, 12, 13]. Indeed, for the Born contribution the corresponding **Im** part is generated by the singularity of $T_0(Q^2, -\sigma; y)$ (multiplied by a power of logarithms), while for the RG summed radiative corrections, one term originates from the **Im** ($\bar{a}_s^{\nu_n}(-\sigma\bar{y} + Q^2 y)/\pi$) contribution.

2.1 Key element of the radiative corrections

The general expression for the key perturbative element follows from the first term in Eq. (4)

$$\begin{aligned}
 & T_0(Q^2, q^2; y) (\bar{a}_s^{\nu_n}(y)) \otimes \psi_n(y) \xrightarrow{q^2 \rightarrow -\sigma} \\
 & \frac{1}{\pi} \int_{m^2}^{\infty} d\sigma \frac{\mathbf{Im}[T_0(Q^2, -\sigma; y) \bar{a}_s^{\nu_n}(-\sigma\bar{y} + Q^2 y)]}{\sigma + q^2} \otimes \psi_n(y) = I_n(Q^2, q^2) \quad (7) \\
 & = \frac{1}{\pi} \int_{m^2}^{\infty} \frac{d\sigma}{\sigma + q^2} \left\{ \mathbf{Re}[T_0(Q^2, -\sigma; y)] \mathbf{Im}[\bar{a}_s^{\nu_n}(-\sigma\bar{y} + Q^2 y)] + \right. \\
 & \quad \left. \mathbf{Im}[T_0(Q^2, -\sigma; y)] \mathbf{Re}[\bar{a}_s^{\nu_n}(-\sigma\bar{y} + Q^2 y)] \right\} \otimes \psi_n(y) \\
 & = \frac{1}{\pi} \int_{m^2}^{\infty} d\sigma \frac{\mathbf{Re}[T_0(Q^2, -\sigma; y)] \mathbf{Im}[\bar{a}_s^{\nu_n}(-\sigma\bar{y} + Q^2 y)]}{\sigma + q^2} \otimes \psi_n(y) + \mathbf{0} \otimes \psi_n(y). \quad (8)
 \end{aligned}$$

Now we impose a new condition: We consider the low limit in the dispersion integral on the RHS, $m^2 \geq 0$, to be the threshold of particle production. This condition affects the outcome of the LCSR even at the level of the Born contribution as we will discuss shortly and marks a crucial difference from our approach in [3]. Phenomenologically, m^2 can be taken to be $m^2 = (2m_\pi)^2 \approx 0.078 \text{ GeV}^2$, or one can treat it as a fit parameter. In Eq. (8) only the first term survives, while the second term vanishes. After the decomposition of the nominator $T_0(Q^2, -\sigma; y) \sim 1/(-\sigma\bar{y} + Q^2 y)$ and the denominator $\sigma + q^2$ in the integrand and by replacing there the variables $\sigma \rightarrow s = -(-\sigma\bar{y} + Q^2 y) \geq 0$, one can derive the integral

$$I_n(Q^2, q^2) = - \int_{m(y)}^{\infty} ds \frac{\rho_{\nu_n}(s)}{s(s + Q(y))} \otimes \psi_n(y), \quad (9a)$$

$$\text{where } \rho_{\nu}(s) = \frac{1}{\pi} \mathbf{Im}[\bar{a}_s^{\nu}(-s - i\varepsilon)]; \quad Q(y) \equiv q^2\bar{y} + Q^2 y; \quad m(y) = m^2\bar{y} - Q^2 y. \quad (9b)$$

The value of the low limit $m(y) > 0$ leads to a new constraint for the integration over s . By contrast, taking $m(y) \leq 0$, one should start to integrate with $s = 0$, where $\rho_{\nu}(s) \neq 0$. Hence we have

$$\begin{aligned}
 I_n(Q^2, q^2) &= - \left[\theta(m(y) > 0) \int_{m(y)}^{\infty} ds \frac{\rho_{\nu_n}(s)}{s(s + Q(y))} + \theta(m(y) \leq 0) \int_0^{\infty} ds \frac{\rho_{\nu_n}(s)}{s(s + Q(y))} \right] \otimes \psi_n(y), \\
 &= - \left[\theta(m(y) > 0) J_{\nu_n}(m(y), Q(y)) + \theta(m(y) \leq 0) J_{\nu_n}(0, Q(y)) \right] \otimes \psi_n(y). \quad (10)
 \end{aligned}$$

The new terms $-J_{\nu}$, introduced on the RHS of Eq. (10), can be decomposed by means of the new coupling \mathcal{I}_{ν} and the previous FAPT couplings $\mathcal{A}_{\nu}, \mathfrak{A}_{\nu}$ to obtain

$$-J_{\nu}(y, x) = - \int_y^{\infty} ds \frac{\rho_{\nu}(s)}{s(s+x)} = \frac{1}{x} [I_{\nu}(y, x) - \mathfrak{A}_{\nu}(y)], \quad (11a)$$

$$\mathcal{I}_{\nu}(y, x) \stackrel{\text{def}}{=} \int_y^{\infty} \frac{d\sigma}{\sigma+x} \rho_{\nu}^{(l)}(\sigma), \quad (11b)$$

$$\mathcal{A}_{\nu}(x) = I_{\nu}(y \rightarrow 0, x), \quad \mathfrak{A}_{\nu}(y) = I_{\nu}(y, x \rightarrow 0), \quad I_1(y \rightarrow 0, x \rightarrow 0) = \mathcal{A}_1(0) = \mathfrak{A}_1(0). \quad (11c)$$

Substituting Eq. (11a) into Eq. (10), one arrives at the final expression for I_n , notably,

$$I_n(Q^2, q^2) = T_0(Q^2, q^2; y) \left\{ [I_\nu(m(y), Q(y)) - \mathfrak{A}_\nu(m(y))] \theta(y < \alpha/(1 + \alpha)) \right. \\ \left. + [\mathcal{A}_\nu(Q(y)) - \mathfrak{A}_\nu(0)] \theta(y \geq \alpha/(1 + \alpha)) \right\} \otimes \psi_n(y), \quad (12)$$

where $\alpha = m^2/Q^2$ and the former couplings appear as the limit of the expressions I_ν in their arguments, cf. (11c). Note that the appearance of coupling differences in the square brackets in Eq. (12) follows from the decomposition in the integrand on the RHS of Eq. (11a).

Turn now to the spectral density. For this we use the standard FAPT expression for the spectral density ρ_ν , i.e.,

$$\rho_\nu^{(l)}(\sigma) = \frac{1}{\pi} \mathbf{Im} [a_{(l)}^\nu(-\sigma)] = \frac{1}{\pi} \frac{\sin[\nu \varphi_{(l)}(\sigma)]}{(R_{(l)}(\sigma))^\nu} \xrightarrow{\text{l-loop}} \frac{1}{\pi} \frac{\sin[\nu \arccos(L_\sigma / \sqrt{L_\sigma^2 + \pi^2})]}{\beta_0^\nu [\pi^2 + L_\sigma^2]^{\nu/2}},$$

where the phase $\varphi_{(l)}$ and the radial part $R_{(l)}$ have a l -loop content, see [7] for details, and $L_\sigma = \ln(\sigma/\Lambda_{\text{QCD}}^2)$. In the equations above, \mathfrak{A}_ν and \mathcal{A}_ν are the standard FAPT couplings for the timelike [7] and spacelike [6] regions, respectively, while the integral $I_\nu(y, x)$ is the new two-parameter coupling in FAPT, introduced in [3], and represents a generalization of the previous FAPT couplings,

$$I_\nu(y, x) = \int_y^\infty \frac{ds}{s+x} \rho_\nu(s) = \mathcal{A}_\nu(x) - \int_0^y \frac{ds}{s+x} \rho_\nu(s) = \mathfrak{A}_\nu(y) - x \int_y^\infty \frac{ds}{s(s+x)} \rho_\nu(s). \quad (13)$$

For our further considerations it is instructive to define an effective coupling \mathbb{A}_ν in terms of the parameter $y_0 = m^2/(m^2 + Q^2)$ as follows

$$\mathbb{A}_\nu(m^2, y) = [\mathcal{A}_\nu(Q(y)) - \mathfrak{A}_\nu(0)] \theta(y \geq y_0) + [I_\nu(m(y), Q(y)) - \mathfrak{A}_\nu(m(y))] \theta(y < y_0). \quad (14)$$

Tuning α to larger values, the second term in (14) becomes more dominant. On the other hand, in the vicinity of y_0 for $m(y_0) = 0$, $\mathbb{A}_\nu(m^2, y)$ is a continuous function by virtue of the properties (11c). To derive practical results, we use the non-threshold approximation $\mathbb{A}_\nu(0, y) \rightarrow [\mathcal{A}_\nu(Q(y)) - \mathfrak{A}_\nu(0)]$ obtained for $m^2 \rightarrow 0$.

2.2 Pion-photon TFF in FAPT

We show the results for the TFF $F_{\text{FAPT}}^{(\text{tw}=2)}(Q^2; m^2)$, obtained from Eq. (4), by taking into account definition (14) of the effective coupling \mathbb{A}_ν in the limits $q^2 \rightarrow 0$, $Q(y) \rightarrow yQ^2$, and $m^2 \geq 0$ in the following explicit form

$$\nu(n=0) = 0; \quad Q^2 F_{\text{FAPT},0}^{(\text{tw}=2)} \equiv F_0(Q^2; m^2) = N_T \left\{ \int_0^1 \frac{\psi_0(x)}{x} dx \right. \\ \left. + \left(\frac{\mathbb{A}_1(m^2, y)}{y} \right) \otimes_y \mathcal{T}^{(1)}(y, x) \otimes_x \psi_0(x) \right\}, \quad (15a)$$

$$\nu(n \neq 0) \neq 0; \quad Q^2 F_{\text{FAPT},n}^{(\text{tw}=2)} \equiv F_n(Q^2; m^2) = \\ \frac{N_T}{a_s^{\nu_n}(\mu^2)} \left\{ \left(\frac{\mathbb{A}_{\nu_n}(m^2, y)}{y} \right) \otimes_y \psi_n(y) + \left(\frac{\mathbb{A}_{1+\nu_n}(m^2, y)}{y} \right) \otimes_y \mathcal{T}^{(1)}(y, x) \otimes_x \psi_n(x) \right\}. \quad (15b)$$

These equations can be related to the initial expressions given by Eqs. (4) by means of the replacement $\mathbb{A}_\nu(m^2, y) \rightarrow \bar{a}_s^\nu(y)$. The advantage of Eqs. (15) is that it does not contain Landau singularities in $\mathbb{A}_{\nu_n}(0, y)$, in contrast to Eq. (4), making it possible to integrate over y . As it was discussed in detail in [3], the singularities of the FAPT couplings do not disappear

completely, but reveal themselves at the end point $Q^2 = 0$ for specific values of the index $0 < \nu < 1$. On the other hand, the magnitude $\mathcal{A}_1^{(1)}(0) = \mathfrak{A}_1(0) = 1/\beta_0$ disturbs the asymptotic value $\sqrt{2}f_\pi$ of the TFF in (15a). Therefore, to save the meaning of the effective coupling \mathbb{A}_ν in (14), we have proposed in [3] ‘‘calibration conditions’’ for $\mathcal{A}_\nu^{(1)}(Q^2)$, $\mathfrak{A}_\nu^{(1)}(Q^2)$ at the origin

$$\mathcal{A}_\nu(0) = \mathfrak{A}_\nu(0) = 0 \quad \text{for } 0 < \nu \leq 1. \quad (16)$$

3 Pion TFF in the FAPT/LCSR approach and comparison with experiment

3.1 FAPT/LSRs for the pion-photon TFF at work

The rearranged perturbative series expansion for the LCSRs via FAPT leads to the new effective couplings $\mathbb{A}_\nu(m^2 = 0, s_0; x)$ (‘‘hard part’’) and $\Delta_\nu(m^2 = 0, x)$ (‘‘resonance part’’) of the LCSRs, where we have taken the limit $m^2 = 0$. These effective couplings consist of the same initial FAPT couplings, like in definition (14), and possess the same structure, despite the low threshold $m^2 = 0$. This should not surprise us, given that the LCSR employs a photon-meson model that involves only a single parameter, namely, the threshold s_0 , i.e., the duality interval for the vector channel,

$$\begin{aligned} \mathbb{A}_\nu(0, s_0; x) &= \theta(x \geq x_0) [\mathcal{A}_\nu(Q(x)) - \mathfrak{A}_\nu(0)] \\ &\quad + \theta(x < x_0) [\mathcal{I}_\nu(s_0(x), Q(x)) - \mathfrak{A}_\nu(s_0(x))] , \end{aligned} \quad (17)$$

$$\begin{aligned} \mathbb{A}_\nu(0; x) - \mathbb{A}_\nu(0, s_0; x) &= \theta(x < x_0) \Delta_\nu(0, x) , \\ \Delta_\nu(0, x) &= [\mathcal{A}_\nu(Q(x)) - \mathcal{I}_\nu(s_0(x), Q(x)) + \mathfrak{A}_\nu(s_0(x)) - \mathfrak{A}_\nu(0)] , \end{aligned} \quad (18)$$

where $s_0(x) = s_0\bar{x} - Q^2x$ (in close analogy to Eq. (9b) for $m(y)$), $x_0 = s_0/(s_0 + Q^2)$. We will not derive here the LCSR for the TFF, recommending for further reading Sec. IV in [3]. We present instead the final results for the partial expressions, see Eq.(3b), pertaining to $F_{\text{LCSR};n}^{\gamma\pi}$

$$F_{\text{LCSR}}^{\gamma\pi}(Q^2) = F_{\text{LCSR};0}^{\gamma\pi}(Q^2) + \sum_{n=2,4,\dots} a_n(\mu^2) F_{\text{LCSR};n}^{\gamma\pi}(Q^2), \quad (19)$$

$$Q^2 F_{\text{LCSR};0}^{\gamma\pi}(Q^2) = N_T \left\{ \int_0^{\bar{x}_0} \bar{\rho}_0(Q^2, x) \frac{dx}{\bar{x}} + \frac{Q^2}{m_\rho^2} \int_{\bar{x}_0}^1 \exp\left(\frac{m_\rho^2}{M^2} - \frac{Q^2}{M^2} \frac{\bar{x}}{x}\right) \bar{\rho}_0(Q^2, x) \frac{dx}{x} \right. \quad (20a)$$

$$\begin{aligned} &+ \left(\frac{\mathbb{A}_1(0, s_0; x)}{x} \right)_x \otimes \mathcal{T}^{(1)}(x, y)_y \otimes \psi_0(y) \\ &+ \left. \frac{Q^2}{m_\rho^2} \int_{\bar{x}_0}^1 \exp\left(\frac{m_\rho^2}{M^2} - \frac{Q^2}{M^2} \frac{\bar{x}}{x}\right) \frac{dx}{x} \Delta_1(0, \bar{x}) \mathcal{T}^{(1)}(\bar{x}, y)_y \otimes \psi_0(y) + O(\mathbb{A}_2) \right\}, \end{aligned} \quad (20b)$$

$$\begin{aligned} Q^2 F_{\text{LCSR};n}^{\gamma\pi}(Q^2) &= \frac{N_T}{a_s^n(\mu^2)} \left\{ \left(\frac{\mathbb{A}_{\nu_n}(0, s_0; x)}{x} \right)_x \otimes \psi_n(x) + \left(\frac{\mathbb{A}_{1+\nu_n}(0, s_0; x)}{x} \right) \right. \\ &\quad \otimes \mathcal{T}^{(1)}(x, y)_y \otimes \psi_n(y) \\ &\quad + \frac{Q^2}{m_\rho^2} \int_{\bar{x}_0}^1 \exp\left(\frac{m_\rho^2}{M^2} - \frac{Q^2}{M^2} \frac{\bar{x}}{x}\right) \frac{dx}{x} \\ &\quad \left. \times \left[\Delta_{\nu_n}(0, \bar{x}) \psi_n(x) + \Delta_{1+\nu_n}(0, \bar{x}) \mathcal{T}^{(1)}(\bar{x}, y)_y \otimes \psi_n(y) \right] + O(\mathbb{A}_2) \right\}. \end{aligned} \quad (20c)$$

In Eq. (20a) we have included in the zero-harmonic spectral density $\bar{\rho}_0$ the contributions stemming from the twist-four and twist-six terms. The latter term was first derived in [13] and reads

$$\begin{aligned}\bar{\rho}_0(Q^2, x) &= \psi_0(x) + \frac{\delta_{\text{tw-4}}^2(Q^2)}{Q^2} x \frac{d}{dx} \varphi^{(4)}(x) + \bar{\rho}_{\text{tw-6}}(Q^2, x), \\ \varphi^{(4)}(x) &= \frac{80}{3} x^2 (1-x)^2; \delta_{\text{tw-4}}^2(Q^2) = \left[\frac{a_s(Q^2)}{a_s(\mu_0^2)} \right]^{\frac{\gamma_{\text{tw-4}}}{\beta_0}} \delta_{\text{tw-4}}^2(\mu_0^2), \gamma_{\text{tw-4}} = 32/9, \\ \bar{\rho}_{\text{tw-6}}(Q^2, x) &= 8\pi \frac{\alpha_s \langle \bar{q}q \rangle^2}{f_\pi^2} \frac{C_F}{N_c} \frac{x}{Q^4} \left[-\left(\frac{1}{1-x} \right)_+ + (2\delta(\bar{x}) - 4x) + x(3 + 2 \ln(x\bar{x})) \right].\end{aligned}\quad (22)$$

Let us conclude this discussion by making two important remarks with regard to the TFF from the FAPT/LCSRs in (20): (i) Any N²LO contribution to Eqs. (20b), (20c) of order $O(\mathbb{A}_{2+\nu})$ is expected to be sufficiently small due to the reason that $\mathcal{A}_2, \mathfrak{A}_2$ are in the domain $Q^2 \lesssim 1 \text{ GeV}^2$ one order of magnitude smaller than $\mathcal{A}_1, \mathfrak{A}_1$ [7]. (ii) For the numerical calculations of the pion-photon TFF to follow, we replace the δ -model of the resonances in (20) with a more realistic Breit-Wigner model [1, 12].

3.2 Numerical results for the TFF and comparison with the experimental data

We show in Fig. 1 predictions for the TFF based on (19), obtained in two different approaches to include the QCD radiative corrections using the LCSR method:

- 1) FAPT/LCSRs from Eq. (20)—black curve.
- 2) FOPT/LCSRs from the results in [2]—blue curve.

In both cases we employ the family of the bimodal BMS pion DAs obtained in [14]. For their parametrization it is sufficient to employ in the Gegenbauer decomposition (3a) the coefficients $\{1, a_2, a_4\}$ derived and discussed in [2, 14, 15]. The shown predictions are calculated using the coefficient values at the normalization scale $\mu^2 \approx 1 \text{ GeV}^2$ [16, 17], viz., $\{a_2(\mu^2) = 0.20(+0.05/-0.06), a_4(\mu^2) = -0.14(+0.09/-0.07), \dots\}$ ¹. The other LCSR parameters have been fixed in previous investigations [1, 2] to be $s_0 \approx 1.5 \text{ GeV}^2$, $M^2 \approx 0.9 \text{ GeV}^2$, $m_\rho^2 \approx 0.6 \text{ GeV}^2$, $\Lambda_{(4)}^{(1-\text{loop})} \approx 0.3 \text{ GeV}$, $\delta_{\text{tw-4}}^2(\mu^2) \approx \lambda_q^2/2 \approx 0.19 \text{ GeV}^2$ and are not varied here. On the other hand, the scale of the twist-six contribution in Eq. (22), for both used schemes FAPT/LCSRs and FOPT/LCSRs is fixed at the admissible upper limit of the condensate $\langle \bar{q}q \rangle^2 = (0.25)^6 \text{ GeV}^6$, see, e.g., [13].

Using Eq. (19) and the partial TFF terms $F_{\text{LCSR};n}^{\gamma\pi}$ from Eqs. (20), we obtain for $Q^2 F_{\text{FAPT}}^{\gamma\pi}(Q^2)$ the prediction shown by the solid black line for the BMS DA in Fig. 1. The (green) strip enveloping this curve indicates the estimated range of theoretical variations of the BMS DA in terms of a_2 and a_4 , while other uncertainties are not considered here. The blue line in this figure corresponds to the FOPT predictions $Q^2 F_{\text{FOPT}}^{\gamma\pi}(Q^2)$ taken at the order N²LO β_0 within the LCSR scheme in [2]. Note that the radiative corrections are negative and become too large in magnitude below about 1 GeV². Obviously, the RG summation effect on the radiative corrections to the TFF provides a good agreement between the FAPT/LCSR TFF predictions and the preliminary BESIII data [10] even in this very low Q^2 domain, where FOPT turns out to be unreliable. This is remarkable, given that the experimental margin of error is very small in this range. The high- Q^2 behavior of the TFF within the FAPT/LCSR approach will be considered elsewhere, while such predictions at the level N²LO within FOPT/LCSRs can be found in [11] with emphasis on the QCD asymptotic limit, denoted in Fig. 1 by the dashed horizontal line.

¹ The values a_2 and a_4 are strongly correlated approximately along the line $a_2 + a_4 = \text{const}$.

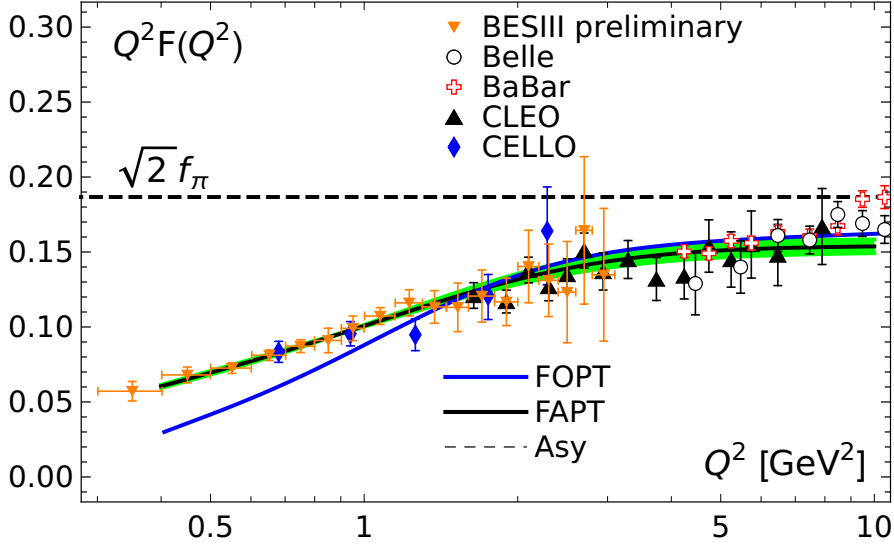


Figure 1. The solid black line and the green strip around it are FAPT predictions for $Q^2 F_{\text{FAPT/LCSR}}^{\gamma\pi}$, whereas the blue line denotes the FOPT prediction for $Q^2 F_{\text{FOPT/LCSR}}^{\gamma\pi}$ at the $N^2\text{LO}$. The experimental data of different collaborations are shown in the upper part of the figure. The single fitted parameter is the scale of the twist-six parameter fixed to the value $\alpha_s \langle \bar{q}q \rangle^2$ defined at its upper bound $\langle \bar{q}q \rangle^2 = (0.25)^6 \text{ GeV}^6$.

4 Conclusion

We considered the lightcone sum-rule description of the pion-photon transition form factor in combination with the renormalization group of QCD and compared the obtained TFF predictions with the corresponding fixed-order results. We showed that the LCSR method, augmented with the RG summation of radiative corrections, naturally leads to a version of fractional analytic perturbation theory that is free of Landau singularities and provides the possibility to include QCD radiative corrections in a resummed way [3]. This FAPT/LCSR approach extends the domain of applicability of the QCD calculation well below 1 GeV^2 and amounts to a significantly smaller total contribution of radiative corrections in this regime relative to a fixed-order calculation. To ensure the compliance with the correct QCD asymptotics of the form factor, new boundary conditions on the FAPT couplings at the origin, $\mathcal{A}_\nu(Q^2 = 0) = \mathfrak{A}_\nu(Q^2 = 0) = 0$, for $0 < \nu \leq 1$, have to be imposed. The FAPT/LCSR approach is best-suited for a detailed comparison with the expected final BESIII data that bear very small errors in the domain below 1 GeV^2 . In fact, as one sees from Fig. 1, the TFF calculated with the family of endpoint-suppressed BMS DAs [14], already agrees with the preliminary BESIII data very well. On the other hand, the TFF results for the BMS DAs within the FOPT/LCSR scheme agree with all data compatible with scaling at high- Q^2 values, where radiative corrections can be reliably computed using FOPT [11].

Acknowledgments

S. V. M. acknowledges support from BelRFFR-JINR, Grant No. F18D-002. A. V. P. was supported by the Chinese Academy of Sciences, President's International Fellowship Initiative (PIFI Grant No. 2019PM0036).

References

- [1] A. Khodjamirian, Eur. Phys. J. **C6**, 477 (1999), hep-ph/9712451
- [2] S.V. Mikhailov, A.V. Pimikov, N.G. Stefanis, Phys. Rev. **D93**, 114018 (2016), 1604.06391
- [3] C. Ayala, S.V. Mikhailov, N.G. Stefanis, Phys. Rev. **D98**, 096017 (2018), 1806.07790
- [4] A.V. Efremov, A.V. Radyushkin, Theor. Math. Phys. **42**, 97 (1980)
- [5] G.P. Lepage, S.V. Brodsky, Phys. Rev. **D22**, 2157 (1980)
- [6] A.P. Bakulev, S.V. Mikhailov, N.G. Stefanis, Phys. Rev. **D72**, 074014 (2005), [Erratum: Phys. Rev. D72, 119908 (2005)], hep-ph/0506311
- [7] A.P. Bakulev, S.V. Mikhailov, N.G. Stefanis, Phys. Rev. **D75**, 056005 (2007), [Erratum: Phys. Rev. D77, 079901 (2008)], hep-ph/0607040
- [8] A.P. Bakulev, Phys. Part. Nucl. **40**, 715 (2009), 0805.0829
- [9] N.G. Stefanis, Phys. Part. Nucl. **44**, 494 (2013), 0902.4805
- [10] C.F. Redmer (BESIII), *Measurement of meson transition form factors at BESIII*, in *13th Conference on the Intersections of Particle and Nuclear Physics (CIPANP 2018) Palm Springs, California, USA, May 29-June 3, 2018* (2018), 1810.00654
- [11] N.G. Stefanis, hep-ph/1904.02631
- [12] S.V. Mikhailov, N.G. Stefanis, Nucl. Phys. **B821**, 291 (2009), 0905.4004
- [13] S.S. Agaev, V.M. Braun, N. Offen, F.A. Porkert, Phys. Rev. **D83**, 054020 (2011), 1012.4671
- [14] A.P. Bakulev, S.V. Mikhailov, N.G. Stefanis, Phys. Lett. **B508**, 279 (2001), [Erratum: Phys. Lett. B590, 309 (2004)], hep-ph/0103119
- [15] N.G. Stefanis, S.V. Mikhailov, A.V. Pimikov, Few Body Syst. **56**, 295 (2015), 1411.0528
- [16] A.P. Bakulev, S.V. Mikhailov, N.G. Stefanis, Phys. Rev. **D67**, 074012 (2003), hep-ph/0212250
- [17] A.P. Bakulev, S.V. Mikhailov, N.G. Stefanis, Annalen Phys. **13**, 629 (2004), hep-ph/0410138